SINGLE DIFFRACTION AND ELASTIC SCATTERING IN PROTON–PROTON COLLISIONS WITH THE STAR DETECTOR AT RHIC*

Mariusz Przybycien

on behalf of the STAR Collaboration

AGH University of Krakow, al. Mickiewicza 30, 30-059 Kraków, Poland

Received 25 November 2024, accepted 7 December 2024, published online 6 March 2025

The diffractive cross sections constitute a significant fraction of the total hadronic cross section in proton–proton collisions. However, due to its non-perturbative nature, the understanding of the fundamental properties of these processes highly relies on experimental studies. In these proceedings, we report on the measurements of the inclusive and identified charged-hadron spectra produced via a single diffraction process in proton–proton collisions at $\sqrt{s} = 200$ GeV. In particular, we compare particle ratios of $\bar{p}/p$ and K/π to theoretical models' calculations. In addition, the first measurement of the proton–proton elastic cross section at $\sqrt{s} = 510$ GeV is presented. The dependences of the elastic cross section on the collision energy and the four-momentum transfer t are discussed and compared to model calculations for the relevant physics implications.

DOI:10.5506/APhysPolBSupp.18.1-A14

1. Introduction

We report on the measurements of the single diffraction (SD) process and elastic scattering in proton–proton (pp) collisions performed by the STAR [1] experiment at RHIC [2]. These two processes, characterized by the presence of one or two intact protons in the final state, are shown schematically in Fig. 1 (left). STAR is especially well suited to perform diffractive-like measurements as it is equipped with the Roman Pot (RP) detection system, which allows for measurements of forward-scattered beam protons at very small angles. The schematic view of the RP system is displayed in Fig. 1 (right), with more details provided in the caption. For more information on the STAR detector, see Ref. [1].

* Presented at the Diffraction and Low-x 2024 Workshop, Trabia, Palermo, Italy, 8–14 September, 2024.

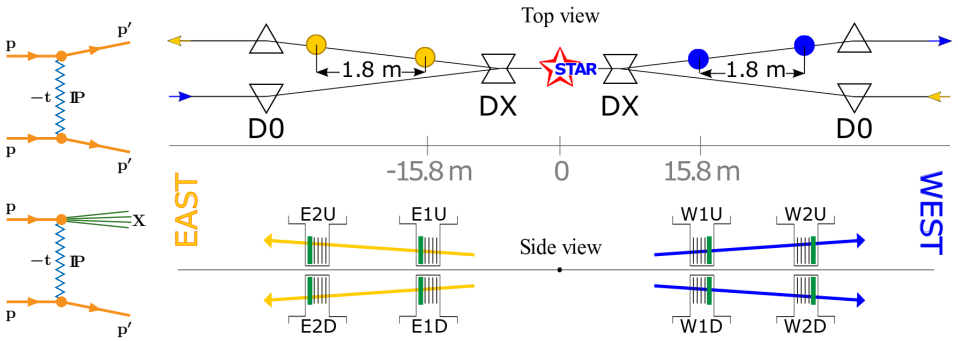

Fig. 1. Left: Diagrams for elastic scattering and single diffractive dissociation in proton–proton scattering. Right: The layout of the RP setup at STAR (not to scale) for measuring forward protons. Top (x, z) and side (y, z) views are shown. Two sets of RPs, labelled (W1, W2) and (E1, E2) were installed between the DX and D0 magnets, at 15.8 m and 17.6 m, on either side of the IP. The detector package has a transverse size of 5×8 cm^2 and a depth of 3.5 cm. The Si sensor is 400 μm thick, while the trigger scintillator is 5 mm thick. The strips in the Si detectors are approximately 100 μm wide. Two dipole magnets, DX and D0, which bend the beams into and out of the IP, are also shown.

2. Single diffraction production of charged hadrons

Production yields of charged hadrons in high-energy particle collisions are among fundamental observables used to study QCD in both perturbative and non-perturbative regimes. Contribution from hard-scattering processes increases with increasing collision energy. However, soft interactions, usually modelled phenomenologically, are the most significant contribution to the number of produced particles. Measurements are necessary to constrain the free parameters of those models, and their good description is crucial for studying other QCD processes at collider experiments, especially at high-luminosity regimes. Several measurements of this type exist in proton–(anti)proton, proton–nucleus, and heavy-ion collisions (see, *e.g.* [3–5]).

Here, we present similar studies for a class of pp collisions in which one of the colliding protons escapes the collision intact at a very small angle and is measured in the RP system. In this SD process, $p+p \to p+X$, X denotes the hadronic final state produced in the interaction due to the dissociation of the other beam proton. Earlier, measurements of this type were performed by the UA4 Collaboration at $\sqrt{s} = 546$ GeV in the proton–antiproton collisions at the CERN SPS collider [6].

Data used in this analysis were collected by the STAR experiment in 2015 in pp collisions at $\sqrt{s} = 200$ GeV and correspond to an integrated luminosity of 15 nb^{-1}. The yields and their ratios discussed here were obtained in

the fiducial region defined by the fractional energy loss of the diffractively scattered proton, $0.02 < \xi < 0.2$, the four-momentum transfer at the proton vertex $0.04 < -t < 0.16$ GeV$^2/c^2$, and the charged particles were required to be produced within $|\eta| < 0.7$ and have $p_{\mathrm{T}} > 0.2$ GeV. The number of charged particles produced in the final state is restricted to $2 \leq n_{\mathrm{ch}} \leq 8$.

STAR has measured multiplicity distributions of charged particles in three ξ intervals. In Fig. 2 (left), the average multiplicity $\langle n_{\mathrm{ch}} \rangle$ in each ξ interval is shown. Data exhibit an expected increase of the $\langle n_{\mathrm{ch}} \rangle$ with ξ due to the larger diffractive masses probed at increasing ξ in the SD process. The shapes of the measured distributions are reproduced reasonably well by all PYTHIA 8 [7] models. The EPOS-LHC [8] (SD+SD′) (here SD′ denotes the EPOS events with a non-diffractive flag, in which only a single proton is produced from the beam remnant) predicts much smaller $\langle n_{\mathrm{ch}} \rangle$ at $\xi < 0.1$ and HERWIG SD [9] predicts for $0.1 < \xi < 0.2$ too large value. It should be noted that EPOS-LHC SD′ describes data much better than EPOS-LHC (SD+SD′).

Densities of charged particles have been also measured as a function of transverse momentum p_{T} in three ξ-intervals. In Fig. 2 (right), the average transverse momentum $\langle p_{\mathrm{T}} \rangle$ in each ξ-interval is shown. Data exhibit no $\langle p_{\mathrm{T}} \rangle$ dependence on ξ. MC models describe data fairly well, predicting $\langle p_{\mathrm{T}} \rangle$ only 0.01 GeV/c higher than in the data except for HERWIG SD, which shows a much steeper dependence of particle density on p_{T} in all three ξ ranges, resulting in significantly lower predictions compared to data.

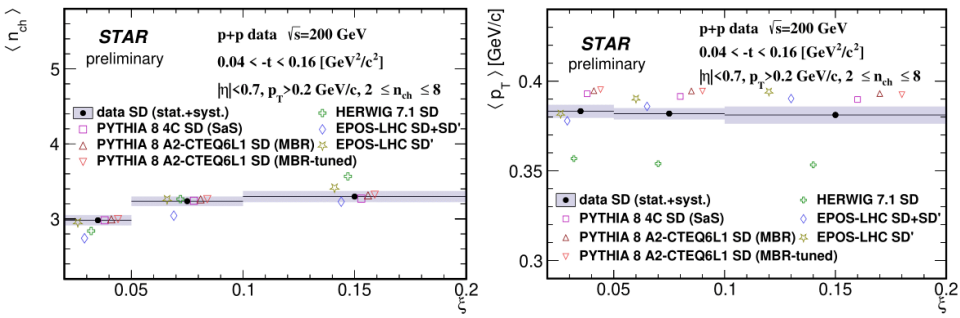

Fig. 2. Mean multiplicity $\langle n_{\mathrm{ch}} \rangle$ (left) and mean transverse momentum $\langle p_{\mathrm{T}} \rangle$ of primary charged particles (right), shown in three ξ intervals. Grey boxes represent statistical and systematic uncertainties added in quadrature. Predictions from MC models, shown as open symbols, are spread within bins for better visibility.

Figure 3 (left) shows the ratios of production yields of $\bar{p}/p$ in three ξ intervals as a function of p_{T}. Data in the last two ξ ranges are consistent with equal amounts of p and $\bar{p}$ with no p_{T} dependence. However, in

the first ξ range at $p_T < 0.7$ GeV, data show a significant deviation from unity, indicating a large transfer of the baryon number from the forward to the central region. The data are compared to several MC models.

Figure 3 (right) shows the ratios of production yields of $(K^- + K^+)/(\pi^- + \pi^+)$ in three intervals of ξ as a function of p_T. The ratio increases from 0.05 at $p_T = 0.3$ GeV to 0.22–0.28 at $p_T = 0.65$ GeV. The slope of the p_T dependence significantly increases at $p_T = 0.5$ GeV in all three ξ intervals. The change in the p_T slope increases with ξ. All models predict similar ratios except HERWIG, which shows values almost twice as large independently of p_T. PYTHIA 8 and EPOS-LHC agree very well with data at $0.3 < p_T < 0.5$ GeV, but do not expect a change in the slope of p_T dependence at $p_T > 0.5$ GeV, predicting rather almost twice the smaller ratio at the highest p_T.

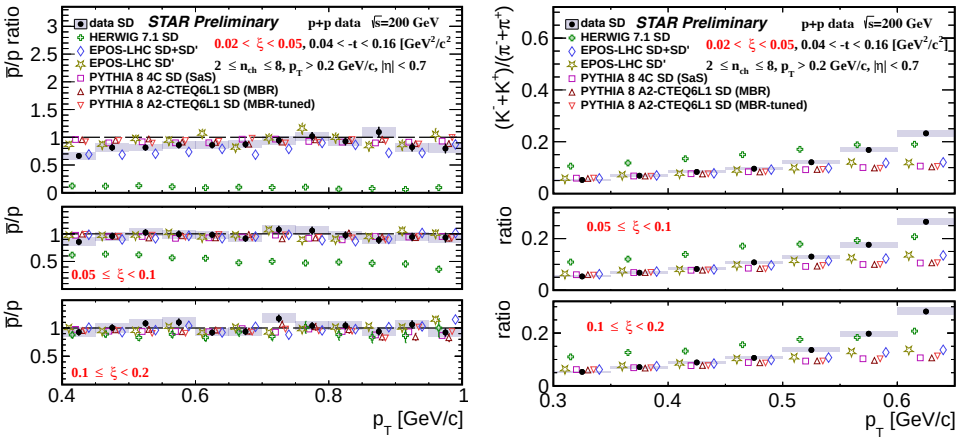

Fig. 3. Ratios of production yields of (left) $\bar{p}/p$ and (right) $(K^- + K^+)/(\pi^- + \pi^+)$, as a function of p_T shown in three ranges of ξ: (top) $0.02 < \xi < 0.05$, (middle) $0.05 < \xi < 0.1$, (bottom) $0.1 < \xi < 0.2$. Data are shown as full dots with error bars representing the statistical uncertainties. Grey boxes represent statistical and systematic uncertainties added in quadrature. Predictions from MC models, shown as open symbols, are spread within bins for better visibility.

3. Elastic cross-section measurement

Recently, STAR published a measurement of the elastic cross section in pp collisions at $\sqrt{s} = 510$ GeV in the four-momentum transfer interval of $0.23 < -t < 0.67$ GeV^2 [10]. The data were acquired in the RHIC 2017 run during the period with special accelerator optics with $\beta^* \approx 8$ m (where β^* is the β-function value at the collision point), which resulted in a beam angular divergence of approximately 30 μrad, which is smaller than that during the standard running conditions. A similar measurement at $\sqrt{s} = 200$ GeV and smaller values of $|t|$ was published by STAR in [11].

The measured elastic cross section is shown in Fig. 4 (left) together with a fit of an exponential function

$$\frac{\mathrm{d}\sigma_{\mathrm{el}}}{\mathrm{d}t} = A \times \exp\left[-B(t)\,|t|\right], \quad \text{where} \quad B(t) = B_0 + B_1\,|t| + B_2\,|t|^2\,.$$

The assumption of the non-constant B was necessary to obtain a reasonable fit. The total elastic cross section in the STAR fiducial region $0.23 < |t| < 0.67$ GeV^2 is $\sigma_{\mathrm{el}}^{\mathrm{fid}} = 462.1 \pm 0.9\,(\mathrm{stat.}) \pm 1.1\,(\mathrm{syst.}) \pm 11.6\,(\mathrm{scale})$ μb, where the scale uncertainty is related to the luminosity determination.

To characterize the shape, we fit a $B = \mathrm{const.}$ slope in six sub-intervals of t range as shown in Fig. 4 (right). The vertical axis is a derivative of the logarithm of the differential cross section $\mathrm{d}(\ln(\mathrm{d}\sigma/\mathrm{d}t))/\mathrm{d}t$, which is a local slope B if one assumes only a constant term in the exponential. There is a good qualitative agreement with the three models shown. In particular, a minimum in $B(t)$ at $-t \approx 0.40$ GeV^2 is observed and predicted.

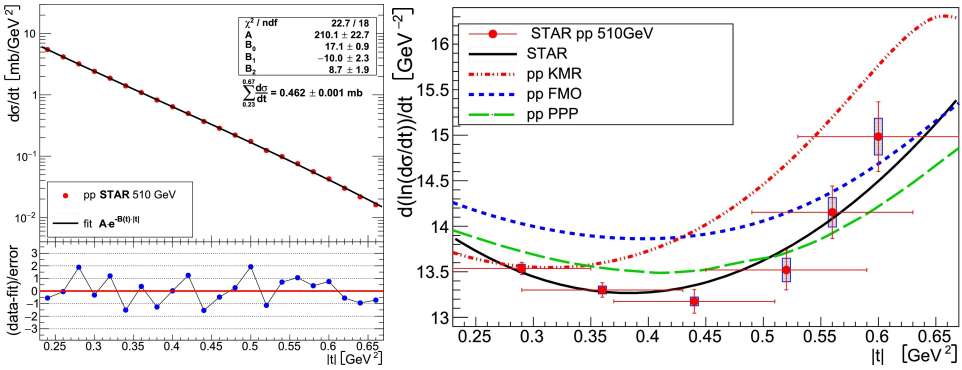

Fig. 4. Left: The pp elastic differential cross section $\mathrm{d}\sigma/\mathrm{d}t$ fitted with an exponential $A \times \exp\left[-B(t)\,|t|\right]$. Bottom panel: Residuals (data–fit)/error. Uncertainties on the data points are smaller than the symbol size. Right: Comparison of the STAR pp results in six t sub-intervals with three models: FMO [12], KMR [13], and PPP [14]. The vertical axis is $\mathrm{d}(\ln(\mathrm{d}\sigma/\mathrm{d}t))/\mathrm{d}t$, which is a local slope B if one assumes only a constant term in the exponential. The black line is a fit for the full data set as described in the text. The horizontal size of the error bars indicates the t range where $B = \mathrm{const.}$ was fitted. The vertical size of the shaded rectangles indicates the systematic uncertainty of the data points.

4. Summary and the future perspective

The STAR experiment used its distinct capability to tag diffractive-like events by directly measuring forward-scattered protons in the RP system to provide new results on elastic scattering and single diffraction. The diffractive data collected by STAR will allow for new, interesting measurements.

This work was partly supported by the National Science Centre (NCN), Poland under grant UMO-2018/30/M/ST2/00395.

REFERENCES

[1] STAR Collaboration (K.H. Ackermann *et al.*), *Nucl. Instrum. Methods Phys. Res. A* **499**, 624 (2003).

[2] H. Hahn *et al.*, *Nucl. Instrum. Methods Phys. Res. A* **499**, 245 (2003).

[3] UA1 Collaboration (G. Arnison *et al.*), *Phys. Lett. B* **123**, 108 (1983).

[4] STAR Collaboration (J. Adams *et al.*), *Phys. Rev. Lett.* **91**, 172302 (2003), arXiv:nucl-ex/0305015.

[5] ATLAS Collaboration (G. Aad *et al.*), *Phys. Lett. B* **758**, 67 (2016), arXiv:1602.01633 [hep-ex].

[6] UA4 Collaboration (M. Bozzo *et al.*), *Phys. Lett. B* **136**, 217 (1984).

[7] T. Sjöstrand *et al.*, *Comput. Phys. Commun.* **178**, 852 (2008), arXiv:0710.3820 [hep-ph].

[8] T. Pierog *et al.*, *Phys. Rev. C* **92**, 034906 (2015), arXiv:1306.0121 [hep-ph].

[9] J. Bellm *et al.*, arXiv:1705.06919 [hep-ph].

[10] STAR Collaboration (M.I. Abdulhamid *et al.*), *Phys. Lett. B* **852**, 138601 (2024), arXiv:2309.16622 [hep-ex].

[11] STAR Collaboration (J. Adam *et al.*), *Phys. Lett. B* **808**, 135663 (2020), arXiv:2003.12136 [hep-ex].

[12] E. Martynov, B. Nicolescu, *Eur. Phys. J. C* **79**, 461 (2019), arXiv:1808.08580 [hep-ph].

[13] V.A. Khoze, A.D. Martin, M.G. Ryskin, *Phys. Lett. B* **784**, 192 (2018), arXiv:1806.05970 [hep-ph].

[14] V.A. Petrov, E. Predazzi, A. Prokudin, *Eur. Phys. J. C* **28**, 525 (2003), arXiv:hep-ph/0206012.